CHEMISTRY
A European Journal

A Journal of ChemPubSoc Europe

Accepted Article

Title: 15N MRI of SLIC-SABRE hyperpolarized 15N-labelled pyridine and nicotinamide

Authors: Kirill Viktorovich Kovtunov, Alexandra Svyatova, Ivan Skovpin, Nikita Chukanov, Igor Koptyug, Eduard Chekmenev, Jan Hoevener, and Andrey Pravdivtsev

To be cited as: *Chem. Eur. J.* 10.1002/chem.201900430

Link to VoR: http://dx.doi.org/10.1002/chem.201900430

Supported by ACES

WILEY-VCH

10.1002/chem.201900430

WILEY-VCH

^{15}N MRI of SLIC-SABRE hyperpolarized ^{15}N-labelled pyridine and nicotinamide

Alexandra Svyatova,[a, b] Ivan V. Skovpin,[a, b] Nikita V. Chukanov, [a, b] Kirill V. Kovtunov,* [a, b] Eduard Y. Chekmenev,[c, d] Andrey N. Pravdivtsev,[e] Jan-Bernd Hövener[e] and Igor V. Koptyug[a, b]

Abstract: Magnetic Resonance Imaging (MRI) is a powerful non-invasive diagnostic method extensively used in biomedical studies. A significant limitation of MRI is its relatively low signal-to-noise ratio, which can be increased by hyperpolarizing nuclear spins. One promising method is Signal Amplification By Reversible Exchange (SABRE), which employs parahydrogen as a source of hyperpolarization. Recent studies demonstrated the feasibility to improve MRI sensitivity with this hyperpolarization technique. Hyperpolarized ^{15}N nuclei in biomolecules can potentially retain their spin alignment for tens of minutes, providing an extended time window for the utilization of the hyperpolarized compounds. In this work, we demonstrate for the first time that radio-frequency-based SABRE hyperpolarization techniques can be used to obtain ^{15}N MRI of biomolecule 1-^{15}N-nicotinamide. Two image acquisition strategies were utilized and compared: Single Point Imaging (SPI) and Fast Low Angle SHot (FLASH). These methods demonstrated opportunities of high-field SABRE for biomedical applications.

Signal Amplification By Reversible Exchange[1] (SABRE) is a rapidly developing parahydrogen-based hyperpolarization approach.[2] Although parahydrogen (pH_2) itself is silent for Nuclear magnetic Resonance (NMR)), simultaneous exchange of pH_2 and the substrate on an Ir-based organometallic complex provides polarization transfer from pH_2–derived hydrides to the substrate, and results in an enhancement of the nuclear spin polarization (P) by several orders of magnitude.[3–7]

[a] A. Svyatova, Dr. I. V. Skovpin, Dr. N. A. Chukanov, Dr. K. V. Kovtunov, Prof. I. V. Koptyug
International Tomography Center, SB RAS
3A Institutskaya st., Novosibirsk 630090, Russia
E-mail: kovtunov@tomo.nsc.ru
[b] A. Svyatova, Dr. I. V. Skovpin, Dr. N. A. Chukanov, Dr. K. V. Kovtunov, Prof. I. V. Koptyug
Novosibirsk State University
2 Pirogova st., Novosibirsk 630090, Russia
[c] Prof. E. Y. Chekmenev
Department of Chemistry
Wayne State University, Karmanos Cancer Institute (KCI), Integrative Biosciences (Ibio)
Detroit, MI 48202, United States
[d] Prof. E. Y. Chekmenev
Russian Academy of Sciences (RAS)
14 Leninskiy Prospekt, Moscow 119991, Russia
[e] Dr. A. N. Pravdivtsev, Prof. Jan-Bernd Hövener
Section Biomedical Imaging, Molecular Imaging North Competence Center (MOIN CC), Department of Radiology and Neuroradiology
University Medical Center Schleswig-Holstein (UKSH), Kiel University,
Am Botanischen Garten 14, 24118 Kiel, Germany

Supporting information for this article is given via a link at the end of the document.

At first, SABRE was demonstrated using pyridine and nicotinamide as substrates.[1] SABRE was performed at magnetic fields of ≈10 mT simply by shaking a sample under pH_2 atmosphere while the signal was acquired later at the high magnetic field of an NMR spectrometer (9.4 T). These simple "shake and run" experiments at low magnetic fields provided high enhancements of the ^{1}H signal by a factor of 550 and 345 for pyridine and nicotinamide, respectively. In addition, ^{1}H MRI of pyridine was obtained with balanced steady-state free precession[8] (b-SSFP) pulse sequence.

In another experiment, SABRE was used to continuously hyperpolarize substrates[9] at a low magnetic field (6.5 mT). This approach was used to enable MRI at Earth's magnetic field. Continuous hyperpolarization[10] resolves the problem of short hyperpolarization lifetimes (T_1-relaxation time is on the order of a few seconds for protons).

The hyperpolarization and imaging of substrates *in situ*, i.e. at the same, constant magnetic field, was shown as well.[11] This approach allowed to accelerate the imaging by shortening the repetition time from 8 s to 0.2 s and to increase the spatial resolution in a way that additional dynamic processes (e.g., pH_2 flow motion) became observable.

Hyperpolarized protons have a relatively short T_1, meanwhile, heteronuclei offer a significantly longer relaxation time. ^{15}N T_1 relaxation values of three to twenty minutes were reported.[12–17] These comparatively long lifetimes significantly increase the time available for sample purification,[18,19] *in vivo* administration, distribution, metabolism and MRI. The first reports of ^{15}N polarization by dissolution DNP[20] show a low efficiency of direct ^{15}N polarization (P~ 4%) with super long build-up times about 2 hours.[13] However, low temperature cross-polarization to nitrogen-15 during dissolution DNP conditions[21] allows to achieve about 20% polarization for urea molecule with moderate build-up times (15 min).[22] Despite the high polarization level, the amount of polarized substance is extremely low (100μL, 0.8M) that along with long build-up times and high cost of DNP instrument limit possible utilization of DNP polarized substances for ^{15}N MRI.

EXPERIMENTAL DESIGN

SABRE showed great potential for heteronuclear MRI: ^{13}C,[1,7,23] ^{15}N,[24] ^{19}F[25,26] and ^{31}P[27,28] images of SABRE polarized substrates were obtained. Here, we focused on ^{15}N nucleus because it can be used in biomedical studies, for example, in pH sensing[24,29] or metabolic imaging.[30–32]

Many SABRE studies were based on polarization transfer at microtesla magnetic fields. These fields are beneficial because polarization transfer to heteronuclei occurs spontaneously in strongly coupled spin systems. The approach based on the use of low magnetic fields was termed SABRE - Shield Enables Alignment Transfer to Heteronuclei (SABRE-SHEATH)[33,34] and

more than 30% ^{15}N-polarization was demonstrated.[18,34,35] However, this approach has two shortcomings:[24,33,35–37] a need of fast magnetic field alteration and creation of polarizer with precise ultralow magnetic field.

In another approach, termed HF-SABRE, the spontaneous polarization transfer from pH_2-derived hydrides to ^{15}N nuclei and MR observation are carryied out *in situ* at a constant, high magnetic field (~10 T).[38] Here, pH_2 is continuously bubbled through the sample, which is placed in the magnet of NMR or MRI, and spontaneous polarization transfer occurs while high-frequency electro-magnetic fields are played out. Although some shortcomings of SABRE-SHEATH were mitigated by HF-SABRE, the ^{15}N-polarization enhancement factors were significantly lower than those provided by SABRE-SHEATH.[38,39]

A previous report on MRI of ^{15}N HF-SABRE[40] revealed that HF-SABRE generates (a relatively low) anti-phase polarization, which is difficult to image due to partial signal cancelation. Therefore, HF-SABRE will likely be limited to *in vitro* imaging and the calibration of hardware or radio-frequency (RF) pulse sequences. Moreover, continuous pH_2 bubbling was required to obtain 2D MRI with extensive signal averaging.

To improve the efficiency of SABRE polarization at high magnetic fields, several polarization transfer techniques employing RF irradiation were developed: Alternating Delays Achieve Polarization Transfer SABRE (ADAPT-SABRE),[41] SABRE Insensitive Nuclei Enhanced by Polarization Transfer (SABRE-INEPT),[42] Low Irradiation Generation of High-Tesla SABRE (LIGHT-SABRE),[43] adiabatic RF-SABRE,[44] Spin Lock Induced Crossing SABRE (SLIC-SABRE),[45] and Quasi-resonance SABRE (QUASR-SABRE).[46] Some of these approaches may deliver ^{15}N HP comparable with the one achieved by SABRE-SHEATH,[46] and also mitigate SABRE-SHEATH shortcomings.

In this work, we present a strategy for performing imaging of SLIC-SABRE hyperpolarized compounds inside an MRI scanner for potential biomedical applications. SLIC-SABRE sequence is an improved version of LIGHT-SABRE where fast singlet – triplet mixing on the Ir-complex is taken into account that makes that variant more robust than LIGHT-SABRE. It was achieved by introduction of a 90° ^{1}H-RF pulse before CW[45] (see Fig. 2, C and Fig. 3, C). Note, that by repeating the SLIC-SABRE block several times polarization is accumulated in the form of free substrate (see **SI**, Fig. S2, B).

Specifically, we hyperpolarized ^{15}N-pyridine (^{15}N-Py) and 1-^{15}N-nicotinamide (^{15}N-NA) via SLIC-SABRE at the high field of an MRI scanner. The parameters for the SLIC-SABRE of ^{15}N-Py were similar to those optimized and reported before: amplitude of RF-pulse, ν_1 = 5 Hz, offset from the center of bound ^{15}N-Py resonance, $\Delta_{rf} \cong$ 17 Hz and duration of continuous wave (CW) RF-pulse, t_{cw} = 1.17 s.[47] For ^{15}N-NA, we used the same parameters of SLIC-SABRE (ν_1, Δ_{rf}, t_{cw}) because when attached to active SABRE-complex it has similar J-coupling constants with hydride protons coming from pH_2. Additionally, we optimized the number of pumping cycles and pH_2 flow rate, as described previously[47] (see Fig. S2, **SI**). All necessary parameters of the experiments are listed in the Tab. S4 (**SI**).

The resulting polarization enhancement factors for free substrate were: ε_{15N} ~ 1,374 for ^{15}N-Py (P ≈ 0.3 %) and ε_{15N} ~ 834 (P ≈ 0.2 %) for ^{15}N-NA at 7 T (Fig. 1). Optimization of the SLIC-SABRE pulse sequence parameters and the calculation of the signal enhancement are given in **SI**. In the Ref.[45] the time period free from RF excitation to refresh system with pH_2 was used, but omitted in this paper. Introduction of such stage can potentially increase the level of hyperpolarization.

The MRI sequence with SABRE polarization consists of the following steps: (i) preparation of hyperpolarization with SLIC-SABRE (this stage can be repeated n times to gain the maximal signal enhancement); (ii) excitation of ^{15}N signal with hard ^{15}N RF pulse; (iii) space encoding; (iv) acquisition of ^{15}N signal. Two different space encoding MRI approaches were used: Single Point Imaging and Fast Low Angle SHot (compare Fig. 2, C and Fig. 3, C).

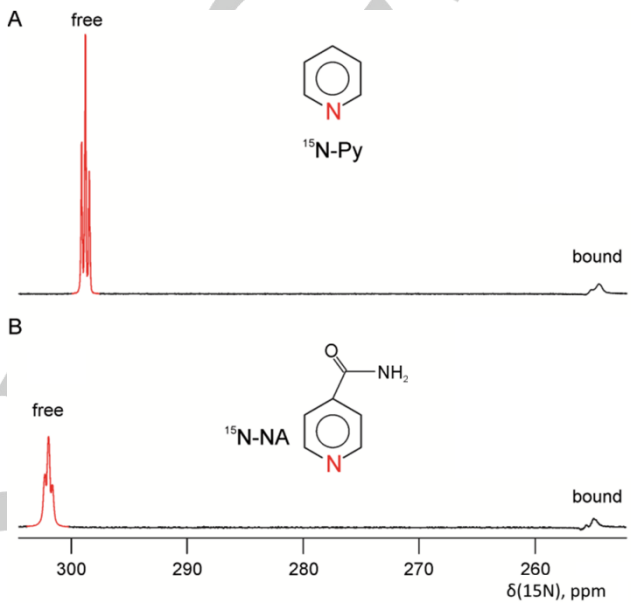

Figure 1. ^{15}N NMR spectra of ^{15}N-Py (A) and ^{15}N-NA (B) hyperpolarized by SLIC-SABRE. Strongly enhanced signals of free and catalyst-bound substrate were observed, enhanced by ε_{15N} ~ 1,374 for ^{15}N-Py and ε_{15N} ~ 834 for ^{15}N-NA (see Fig. S1, **SI**). A pH_2 pressure of 3.4 bar and a flow rate of 80 sccm were used. The experiments were carried out at room temperature. Two different samples were used: 0.1 M ^{15}N-Py and 5 mM Ir(IMes) methanol-d_4 solution (A) and 0.1 M ^{15}N-NA and 5 mM Ir(IMes) methanol-d_4 solution (B).

^{15}N-Single-point MRI enhanced by SLIC-SABRE. High-resolution, 2D Single Point Imaging (SPI) was realized by using two spatial encoding gradients G_x and G_y without slice selection (Fig. 2, C). Each point of k-space was acquired consequently after the SLIC-SABRE pulse sequence, a 90° excitation pulse and two spatial encoding gradients. In total, 16x16=256 points were acquired, resulting in a high native spatial resolution of 565×565 μm^2/pixel. It means that the experiments were repeated 256 times with constant hyperpolarization production. Here we took advantage of SABRE method that allows, unlike DNP, fast and continuous production of hyperpolarization. The gained resolution was sufficient to image the thin, 1/16 inches ≅ 1.6 mm capillary supplying pH_2 to the NMR tube (Fig. 2). Note that the fine details were resolved despite the fact that pH_2 was continuously supplied, which induces convection in the liquid sample. In the context of biomedical applications, however, the scan times of 5.5 minutes (Py) or 27 minutes (NA) are impractical. Moreover, ^{15}N polarization had to be re-created for each point of k-space, which makes the method inherently slow.

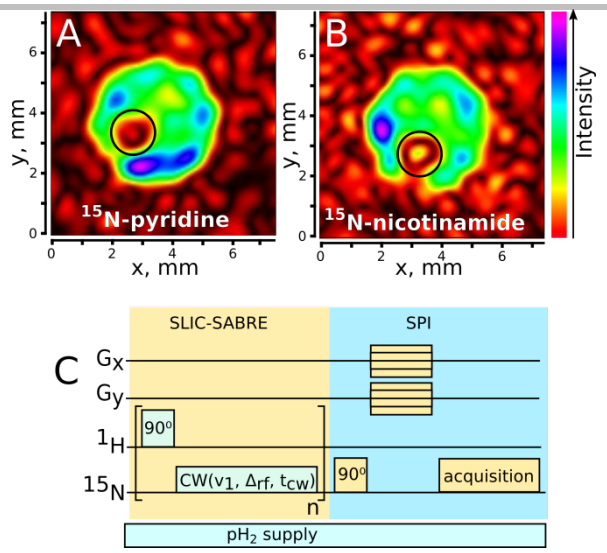

Figure 2. ^{15}N single-point MRI of 0.1 M ^{15}N-Py (A) and 0.1 M ^{15}N-NA (B) in methanol-d_4 with 5 mM Ir(COD)(IMes)Cl hyperpolarized by means of SLIC-SABRE with a 7 sccm pH_2 flow rate at 9.4 T. 2D images were acquired using SLIC-SABRE hyperpolarization and SPI spatial encoding and acquisition elements (C). Total scan time was 5.5 min (A) and 27 min (B). The signal void (circle) corresponds to the pH_2 supply capillary. Experiments were carried out at room temperature. The number of SLIC-SABRE cycles, n, was 1 for ^{15}N-Py and 5 for ^{15}N-NA. In both cases, k-space was acquired once, acquisition spectral width (SW) was 12 kHz, spatial resolution was 565×565 μm^2/pixel. Field of view was 0.9×0.9 cm^2, acquisition matrix was 16×16, It was zero-filled to 128×128 before the image reconstruction.

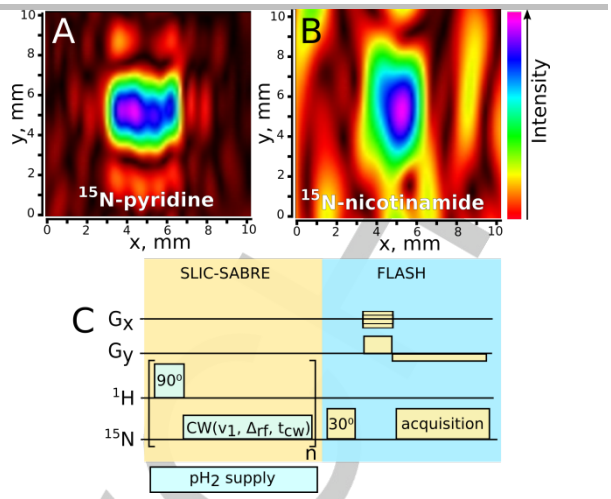

Figure 3. ^{15}N FLASH-MRI of 1 M ^{15}N-Py with 50 mM of Ir(COD)(IMes)Cl (A) and 0.1 M ^{15}N-NA with 5 mM Ir(COD)(IMes)Cl (B) in methanol-d_4 hyperpolarized by SLIC-SABRE with 35 sccm pH_2 flow rate at 9.4 T. 2D images were acquired using SLIC-SABRE hyperpolarization and FLASH spatial encoding and acquisition elements (C). Repetition time (TR) was 3.1 ms, echo time time (TE) was 1 ms. Experiments were carried out at room temperature. The number of SLIC-SABRE pumping cycles, n, was 10 and no signal averaging was employed. Acquisition spectral width (SW) was 10 kHz, spatial resolution was 0.15×2.4 mm^2/pixel (A) and 0.3×4.8 mm^2/pixel (B). Field of view was 1.9×1.9 cm^2 (A) and 3.8×3.8 cm^2 (B), Acquisition matrix was 128×8, it was were zero-filled to matrix size of 128×128 (A) and 256×256 (B) before image reconstruction.

^{15}N-FLASH MRI enhanced by SLIC-SABRE. Using a gradient echo pulse sequence such as Fast Low Angle Shot (FLASH) allows one to decrease the scan time by orders of magnitude. Here, an entire k-space was read out after one SLIC-SABRE block (Fig. 3, C). This is advantageous, because in biomedical conditions, it would be impossible to re-hyperpolarize an injected HP bolus for every excitation, as was done for SPI.

In this setting, the hyperpolarization by SLIC-SABRE took 13 s and the FLASH MRI less than 1 s (repetition time 3.1 ms, echo time 1 ms, 8 phase encoding steps, 128 readout points, Cartesian encoding). There was a delay of approximately 2-4 s between SLIC-SABRE and MRI due to hardware limitations while switching between two pulse sequences. We do not expect significant polarization losses during this delay (see HP decay kinetics in Fig. S3, **SI**). Note that the whole k-space was acquired after only one implementation of SLIC-SABRE.

As a result, ^{15}N images (Fig. 3) were obtained using a 128×8 matrix that provide a spatial resolution of 0.15×2.4 mm^2/pixel (^{15}N-Py) and 0.3×4.8 mm^2/pixel (^{15}N-NA). For representation, the k-space data sets were zero-filled to 128×128 and 256×256 for ^{15}N-Py and ^{15}N-NA, respectively.

Conclusion. The presented approach allowed us to hyperpolarize and image ^{15}N biomolecules inside an MRI instrument, in situ, by SLIC-SABRE in less than a minute. The HP was continuously renewed inside the MRI scanner, which provides certain advantages in the context of biomedical applications.[48] The HP was strong enough to allow subsecond ^{15}N MRI of two ^{15}N-labeled biomolecules: ^{15}N-Py and ^{15}N-NA (vitamin B_3). No external polarizer or sample transfer to an MRI scanner are required.

SLIC-SABRE was introduced as an efficient way to transfer polarization from pH_2 to a ^{15}N substrate. Here, we obtained 1,374- and 834-fold signal enhancements for ^{15}N-Py and ^{15}N-NA, respectively. Although the polarizations are moderate the enhancements are quite significant and sufficient for fast MRI. We expect that future advances in SLIC-SABRE or related methods will increase the polarization further.

While in these studies organic solvents were used and the catalyst was not removed before imaging, recent advances in filtering,[7,18] heterogeneous catalysis [49] and ^{15}N SABRE-SHEATH in aqueous medium[36] bode well for a future *in vivo* translation of the presented approach. The ^{15}N sites can retain HP state for tens of minutes, but their detection sensitivity is approximately two orders of magnitude lower than that of protons. This shortcoming can be mitigated by transferring polarization from ^{15}N to *J*-coupled ^{1}H nuclei and subsequent ^{1}H imaging. Various schemes have been designed for this indirect readout and have already been demonstrated *in vivo*.[50–53]

This work is the first demonstration of hyperpolarized, heteronuclear MRI that was enhanced by SLIC-SABRE rather than by spontaneous polarization transfer. This method can be extended to other heteronuclei such as ^{13}C, ^{19}F, ^{31}P, etc. for biomedical and other applications.

Experimental Section

Iridium N-heterocyclic carbene complexes, Ir(COD)(IMes)Cl (IMes = 1,3-bis(2,4,6-trimethylphenyl)imidazole-2-ylidene, COD = cyclooctadiene) was used as a pre-catalyst to provide SABRE. This complex was prepared from commercially available precursors ($[Ir(COD)Cl]_2$, abcr GmbH, CAS: 12112-67-3; $[IMes]^+[BF_4]^-$, Sigma Aldrich, CAS: 245679-18-9) according to the previously described method.[54,55] Pre-catalyst was activated by bubbling pH_2 through the reagent solution in the presence of a substrate during 20 minutes with pH_2 flow rate of 20 sccm and 1.7 bar overpressure. Activation was required to convert the pre-catalyst to the active SABRE-complex.

^{15}N-pyridine and 1-^{15}N-nicotinamide used as SABRE substrates were synthesized according to the procedures described in the literature (for details of synthesis of ^{15}N-pyridine see **SI**).[56,57] 600 µl methanol-d_4 mixtures: 1 M solution of ^{15}N-Py and 50 mM of Ir(COD)(IMes)Cl, 0.1 M solution of ^{15}N-Py and 5 mM of Ir(COD)(IMes)Cl or 0.1 M solution of ^{15}N-NA and 5 mM Ir(COD)(IMes)Cl, were used for MRI experiments. All experiments were carried out using standard 5 mm NMR tubes. pH_2 was supplied to the solution through the capillary system equipped with a mass flow controller and back pressure valves (Fig. 4). pH_2 was prepared using a commercially available pH_2 generator with a conversion temperature of 38 K that provides ~90% enrichment of the para fraction (Bruker, BPHG90).

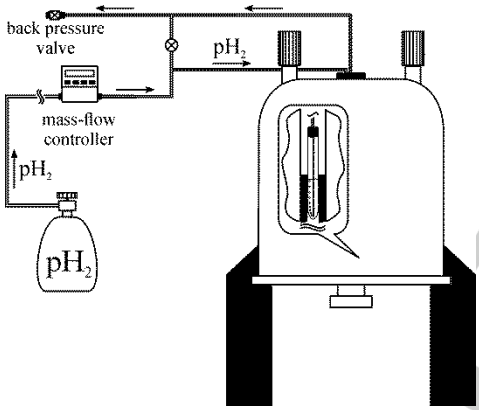

Figure 4. Scheme of the HF-SABRE MR setup. pH_2 was supplied to the sample solution placed inside the spectrometer trough the capillary system. The gas system contained mass flow controller and back pressure valves

MR images were acquired with a 400 MHz (B_0 = 9.4 T) microimaging instrument (Bruker, Avance III) equipped with a two-channel probe (^{1}H, ^{15}N) and maximal gradient strength of 150 G/cm. The SLIC pulse sequence[58] was used to transfer nuclear spin order from pH_2 to ^{15}N in the strong magnetic field.[45,58] NMR spectra were obtained on a 300 MHz (B_0 = 7 T) NMR spectrometer (Bruker, Avance).

^{15}N-Single-point MRI enhanced by SLIC-SABRE. Parahydrogen was delivered to the solution at 1.7 bar and 7 sccm flow rate during SLIC-SABRE and MRI. For SPI, two phase encoding gradients (Fig. 2, C) were applied after non-selective 90° excitation, and each point of k-space was acquired separately after SLIC-SABRE (a total of 16x16). Phase encoding gradients had 45% strength of maximal value and 300 µs duration. 1 or 5 SLIC-SABRE cycles of ca. 1.2 s each were applied for HP of ^{15}N-Py and ^{15}N-NA, respectively.

^{15}N-FLASH MRI enhanced by SLIC-SABRE. For both substrates, SLIC-SABRE (ca. 1.2 s each) was repeated 10 times, resulting in a total duration of 13 s. At the beginning, pH_2 was flushed through the solution with a flow rate of 35 sccm and 3.5 bar pressure. Importantly, the flow of pH_2 was stopped 4-6 s before the onset of the MRI (11 s after the onset of SLIC) to reduce magnetic field inhomogeneities and fast convection caused by the bubbles. There was a delay of approximately 2-4 s between SLIC-SABRE and MRI due to hardware limitations. Duration of the FLASH was less than a second, TR was 3.1 ms, TE was 1 ms. Phase encoding gradient had 8% strength of maximal value and 400 µs duration, readout gradient had 4% strength and 2.1 ms duration. The flip angle was 30°. No k-space filter was applied.

Acknowledgements

A.S., N.V.C., and K.V.K. thank the Russian Science Foundation (grant #17-73-20030) for the support ^{15}N MR imaging experiments of pyridine and nicotinamide. I.V.S and I.V.K thank RFBR (grant # 19-53-12013) for the support of synthesis of ^{15}N-labeled compounds and Ministry of Science and Higher Education of the RF (AAAA-A16-116121510087-5) for access to NMR equipment. E.Y.C thanks the following funding support: NSF under grant CHE-1836308, NIH 1R21EB020323 and R21CA220137, DOD CDMRP W81XWH-12-1-0159/BC112431. A. N. P. and J.-B. H. acknowledge support by the DFG in the Emmy Noether Program (HO 4604/2-1), the Research Training Circle Materials for Brain (GRK 2154), a research grant (HO 4604/3-1), the cluster of excellence "Inflammation at Interfaces" (EXC 306) and precision medicine in inflammation (PMI 1267). Kiel University and the Medical Faculty are acknowledged for supporting the Molecular Imaging North Competence Center (MOIN CC) as a core facility for imaging in vivo. MOIN CC was founded by a grant of the European Regional Development Fund (ERDF) and the Zukunftsprogramm Wirtschaft of Schleswig-Holstein (Project no. 122-09-053).

Keywords: SABRE • ^{15}N MRI • parahydrogen • hyperpolarization • molecular imaging

[1] R. W. Adams, J. A. Aguilar, K. D. Atkinson, M. J. Cowley, P. I. P. Elliott, S. B. Duckett, G. G. R. Green, I. G. Khazal, J. Lopez-Serrano, D. C. Williamson, *Science (80-.).* **2009**, *323*, 1708–1711.
[2] C. R. Bowers, D. P. Weitekamp, *Phys. Rev. Lett.* **1986**, *57*, 2645–2648.
[3] P. Nikolaou, B. M. Goodson, E. Y. Chekmenev, *Chem. - A Eur. J.* **2015**, *21*, 3156–3166.
[4] K. V. Kovtunov, E. V. Pokochueva, O. G. Salnikov, S. F. Cousin, D. Kurzbach, B. Vuichoud, S. Jannin, E. Y. Chekmenev, B. M. Goodson, D. A. Barskiy, et al., *Chem. - An Asian J.* **2018**, *13*, 1857–1871.
[5] D. A. Barskiy, A. N. Pravdivtsev, K. L. Ivanov, K. V. Kovtunov, I. V. Koptyug, *Phys. Chem. Chem. Phys.* **2016**, *18*, 89–93.
[6] J.-B. Hövener, A. N. Pravdivtsev, B. Kidd, C. R. Bowers, S. Glöggler, K. V Kovtunov, M. Plaumann, R. Katz-Brull, K. Buckenmaier, A. Jerschow, et al., *Angew. Chemie Int. Ed.* **2018**, *57*, 11140–11162.
[7] J. B. Hövener, N. Schwaderlapp, R. Borowiak, T. Lickert, S. B. Duckett, R. E. Mewis, R. W. Adams, M. J. Burns, L. A. R. Highton, G. G. R. Green, et al., *Anal. Chem.* **2014**, *86*, 1767–1774.
[8] H. Y. Carr, *Phys. Rev.* **1958**, *112*, 1693–1701.
[9] J.-B. Hövener, N. Schwaderlapp, T. Lickert, S. B. Duckett, R. E. Mewis, L. A. R. Highton, S. M. Kenny, G. G. R. Green, D. Leibfritz, J. G. Korvink, et al., *Nat. Commun.* **2013**, *4*, 2946.
[10] P. Štěpánek, C. Sanchez-Perez, V.-V. Telkki, V. Zhivonitko, A. M. Kantola, *J. Magn. Reson.* **2019**, DOI 10.1016/j.jmr.2019.01.003.
[11] D. A. Barskiy, K. V. Kovtunov, I. V. Koptyug, P. He, K. A. Groome, Q. A. Best, F. Shi, B. M. Goodson, R. V. Shchepin, M. L. Truong, et al., *ChemPhysChem* **2014**, *15*, 4100–4107.
[12] R. Sarkar, A. Comment, P. R. Vasos, S. Jannin, R. Gruetter, G. Bodenhausen, H. Hall, D. Kirik, V. P. Denisov, *J. Am. Chem. Soc.* **2009**, *131*, 16014–16015.
[13] H. Nonaka, R. Hata, T. Doura, T. Nishihara, K. Kumagai, M. Akakabe, M. Tsuda, K. Ichikawa, S. Sando, *Nat. Commun.* **2013**, *4*, 2411.

[14] L. B. Bales, K. V. Kovtunov, D. A. Barskiy, R. V. Shchepin, A. M. Coffey, L. M. Kovtunova, A. V. Bukhtiyarov, M. A. Feldman, V. I. Bukhtiyarov, E. Y. Chekmenev, et al., *J. Phys. Chem. C* **2017**, *121*, 15304–15309.
[15] C. Cudalbu, A. Comment, F. Kurdzesau, R. B. Heeswijk, K. Uffmann, S. Jannin, V. Denisov, D. Kirike, R. Gruetter, *Phys. Chem. Chem. Phys.* **2010**, *12*, 5818–5823.
[16] T. Theis, G. X. Ortiz, A. W. J. Logan, K. E. Claytor, Y. Feng, W. P. Huhn, V. Blum, S. J. Malcolmson, E. Y. Chekmenev, Q. Wang, et al., *Sci. Adv.* **2016**, *2*, e1501438–e1501438.
[17] J. McCormick, S. Korchak, S. Mamone, Y. N. Ertas, Z. Liu, L. Verlinsky, S. Wagner, S. Glöggler, L. S. Bouchard, *Angew. Chemie - Int. Ed.* **2018**, *57*, 10692–10696.
[18] B. E. Kidd, J. L. Gesiorski, M. E. Gemeinhardt, R. V. Shchepin, K. V. Kovtunov, I. V. Koptyug, E. Y. Chekmenev, B. M. Goodson, *J. Phys. Chem. C* **2018**, *122*, 16848–16852.
[19] D. A. Barskiy, L. A. Ke, X. Li, V. Stevenson, N. Widarman, H. Zhang, A. Truxal, A. Pines, *J. Phys. Chem. Lett.* **2018**, *9*, 2721–2724.
[20] K. V. Kovtunov, E. V. Pokochueva, O. G. Salnikov, S. F. Cousin, D. Kurzbach, B. Vuichoud, S. Jannin, E. Y. Chekmenev, B. M. Goodson, D. A. Barskiy, et al., *Chem. - An Asian J.* **2018**, *13*, 1857–1871.
[21] S. Jannin, A. Bornet, R. Melzi, G. Bodenhausen, *Chem. Phys. Lett.* **2012**, *549*, 99–102.
[22] J. Milani, B. Vuichoud, A. Bornet, R. Melzi, S. Jannin, G. Bodenhausen, *Rev. Sci. Instrum.* **2017**, *88*, 15109.
[23] R. E. Mewis, R. A. Green, M. C. R. Cockett, M. J. Cowley, S. B. Duckett, G. G. R. Green, R. O. John, P. J. Rayner, D. C. Williamson, *J. Phys. Chem. B* **2015**, *119*, 1416–1424.
[24] R. V Shchepin, D. A. Barskiy, A. M. Coffey, T. Theis, F. Shi, W. S. Warren, B. M. Goodson, E. Y. Chekmenev, *ACS Sensors* **2016**, *1*, 640–644.
[25] N. V. Chukanov, O. G. Salnikov, R. V Shchepin, A. Svyatova, K. V. Kovtunov, I. V. Koptyug, E. Y. Chekmenev, *J. Phys. Chem. C* **2018**, *122*, 23002–23010.
[26] R. V. Shchepin, B. M. Goodson, T. Theis, W. S. Warren, E. Y. Chekmenev, *ChemPhysChem* **2017**, *18*, 1961–1965.
[27] M. J. Burns, P. J. Rayner, G. G. R. Green, L. A. R. Highton, R. E. Mewis, S. B. Duckett, *J. Phys. Chem. B* **2015**, *119*, 5020–5027.
[28] V. V. Zhivonitko, I. V. Skovpin, I. V. Koptyug, *Chem. Commun.* **2015**, *51*, 2506–2509.
[29] W. Jiang, L. Lumata, W. Chen, S. Zhang, Z. Kovacs, A. D. Sherry, C. Khemtong, *Sci. Rep.* **2015**, *5*, 9104.
[30] C. Gabellieri, S. Reynolds, A. Lavie, G. S. Payne, M. O. Leach, T. R. Eykyn, *J. Am. Chem. Soc.* **2008**, *130*, 4598–4599.
[31] C. Cudalbu, A. Comment, F. Kurdzesau, R. B. van Heeswijk, K. Uffmann, S. Jannin, V. Denisov, D. Kirik, R. Gruetter, *Phys. Chem. Chem. Phys.* **2010**, *12*, 5818.
[32] S. J. Nelson, J. Kurhanewicz, D. B. Vigneron, P. E. Z. Larson, A. L. Harzstark, M. Ferrone, M. van Criekinge, J. W. Chang, R. Bok, I. Park, et al., *Sci. Transl. Med.* **2013**, *5*, 198ra108.
[33] M. L. Truong, T. Theis, A. M. Coffey, R. V. Shchepin, K. W. Waddell, F. Shi, B. M. Goodson, W. S. Warren, E. Y. Chekmenev, *J. Phys. Chem. C* **2015**, *119*, 8786–8797.
[34] T. Theis, M. L. Truong, A. M. Coffey, R. V. Shchepin, K. W. Waddell, F. Shi, B. M. Goodson, W. S. Warren, E. Y. Chekmenev, *J. Am. Chem. Soc.* **2015**, *137*, 1404–1407.
[35] D. A. Barskiy, R. V. Shchepin, A. M. Coffey, T. Theis, W. S. Warren, B. M. Goodson, E. Y. Chekmenev, *J. Am. Chem. Soc.* **2016**, *138*, 8080–8083.
[36] J. F. P. Colell, M. Emondts, A. W. J. Logan, K. Shen, J. Bae, R. V. Shchepin, G. X. Ortiz, P. Spannring, Q. Wang, S. J. Malcolmson, et al., *J. Am. Chem. Soc.* **2017**, *139*, 7761–7767.
[37] A. S. Kiryutin, A. V. Yurkovskaya, H. Zimmermann, H.-M. Vieth, K. L. Ivanov, *Magn. Reson. Chem.* **2018**, *56*, 651–662.
[38] D. A. Barskiy, K. V. Kovtunov, I. V. Koptyug, P. He, K. a. Groome, Q. a. Best, F. Shi, B. M. Goodson, R. V. Shchepin, A. M. Coffey, et al., *J. Am. Chem. Soc.* **2014**, *136*, 3322–3325.
[39] A. N. Pravdivtsev, A. V Yurkovskaya, P. A. Petrov, H. Vieth, *Appl. Magn. Reson.* **2016**, *47*, 711–725.
[40] K. V Kovtunov, B. E. Kidd, O. G. Salnikov, L. B. Bales, M. E. Gemeinhardt, J. Gesiorski, R. V Shchepin, E. Y. Chekmenev, B. M. Goodson, I. V Koptyug, *J. Phys. Chem. C* **2017**, *121*, 25994–25999.
[41] S. S. Roy, G. Stevanato, P. J. Rayner, S. B. Duckett, *J. Magn. Reson.* **2017**, *285*, 55–60.
[42] A. N. Pravdivtsev, A. V. Yurkovskaya, H. Zimmermann, H.-M. Vieth, K. L. Ivanov, *Chem. Phys. Lett.* **2016**, *661*, 77–82.
[43] T. Theis, M. Truong, A. M. Coffey, E. Y. Chekmenev, W. S. Warren, *J. Magn. Reson.* **2014**, *248*, 23–26.
[44] A. N. Pravdivtsev, A. V Yurkovskaya, H. Zimmermann, H. Vieth, K. L. Ivanov, *RSC Adv.* **2015**, *5*, 63615–63623.
[45] S. Knecht, A. S. Kiryutin, A. V. Yurkovskaya, K. L. Ivanov, *Mol. Phys.* **2018**, *0*, 1–10.
[46] T. Theis, N. M. Ariyasingha, R. V. Shchepin, J. R. Lindale, W. S. Warren, E. Y. Chekmenev, *J. Phys. Chem. Lett.* **2018**, *9*, 6136–6142.
[47] A. N. Pravdivtsev, I. V. Skovpin, A. I. Svyatova, N. V Chukanov, L. M. Kovtunova, V. I. Bukhtiyarov, E. Y. Chekmenev, K. V Kovtunov, I. V Koptyug, J.-B. Hövener, *J. Phys. Chem. A* **2018**, *122*, 9107–9114.
[48] A. B. Schmidt, S. Berner, M. Braig, M. Zimmermann, J. Hennig, D. von Elverfeldt, J.-B. Hövener, *PLoS One* **2018**, *13*, e0200141.
[49] K. V. Kovtunov, L. M. Kovtunova, M. E. Gemeinhardt, A. V. Bukhtiyarov, J. Gesiorski, V. I. Bukhtiyarov, E. Y. Chekmenev, I. V. Koptyug, B. M. Goodson, *Angew. Chemie - Int. Ed.* **2017**, *56*, 10433–10437.
[50] M. L. Truong, A. M. Coffey, R. V. Shchepin, K. W. Waddell, E. Y. Chekmenev, *Contrast Media Mol. Imaging* **2014**, *9*, 333–341.
[51] J. Wang, F. Kreis, A. J. Wright, R. L. Hesketh, M. H. Levitt, K. M. Brindle, *Magn. Reson. Med.* **2018**, *79*, 741–747.
[52] V. A. Norton, D. P. Weitekamp, *J. Chem. Phys.* **2011**, *135*, 141107.
[53] E. Y. Chekmenev, V. A. Norton, D. P. Weitekamp, P. Bhattacharya, *J. Am. Chem. Soc.* **2009**, *131*, 3164–3165.
[54] M. J. Cowley, R. W. Adams, K. D. Atkinson, M. C. Cockett, S. B. Duckett, G. G. Green, J. A. Lohman, R. Kerssebaum, D. Kilgour, R. E. Mewis, *J. Am. Chem. Soc.* **2011**, *133*, 6134–6137.
[55] L. D. Vazquez-serrano, B. T. Owens, J. M. Buriak, **2006**, *359*, 2786–2797.
[56] R. V Shchepin, D. A. Barskiy, D. M. Mikhaylov, E. Y. Chekmenev, *Bioconj. Chem.* **2016**, *27*, 878–882.
[57] T. W. Whaley, D. G. Ott, *J. Labelled Compd.* **1974**, *10*, 283–286.
[58] S. J. DeVience, R. L. Walsworth, M. S. Rosen, *Phys. Rev. Lett.* **2013**, *111*, 173002.

10.1002/chem.201900430

WILEY-VCH

Entry for the Table of Contents

COMMUNICATION

^{15}N Signal Amplification By Reversible Exchange hyperpolarization of biomolecules were carried out *in situ* in a MRI scanner. This allowed us to perform ^{15}N MRI of ^{15}N-pyridine and 1-^{15}N-nicotinamide using two different pulse sequences: Single Point Imaging and Fast Low Angle SHot (FLASH). The demonstrated method is a promising approach for biomedical applications.

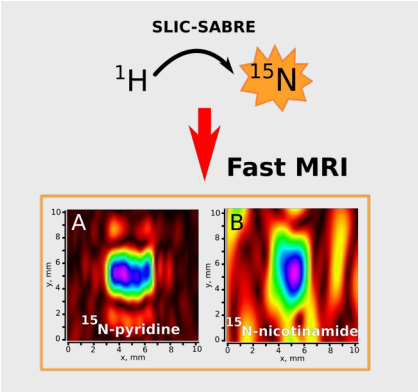

Alexandra Svyatova, Ivan V. Skovpin, Nikita V. Chukanov, Kirill V. Kovtunov, Eduard Y. Chekmenev, Andrey N. Pravdivtsev, Jan-Bernd Hövener, Igor V. Koptyug*

Page No. – Page No.

^{15}N MRI of SLIC-SABRE hyperpolarized ^{15}N-labelled pyridine and nicotinamide